REVIEW / SYNTHÈSE

Mechanistic principles and applications of resonance energy transfer

David L. Andrews

Abstract: Resonance energy transfer is the primary mechanism for the migration of electronic excitation in the condensed phase. Well-known in the particular context of molecular photochemistry, it is a phenomenon whose much wider prevalence in both natural and synthetic materials has only slowly been appreciated, and for which the fundamental theory and understanding have witnessed major advances in recent years. With the growing to maturity of a robust theoretical foundation, the latest developments have led to a more complete and thorough identification of key principles. The present review first describes the context and general features of energy transfer, then focusing on its electrodynamic, optical, and photophysical characteristics. The particular role the mechanism plays in photosynthetic materials and synthetic analogue polymers is then discussed, followed by a summary of its primarily biological structure determination applications. Lastly, several possible methods are described, by the means of which all-optical switching might be effected through the control and application of resonance energy transfer in suitably fabricated nanostructures.

Key words: FRET, Förster energy transfer, photophysics, fluorescence, laser.

Résumé : Dans une phase condensée, le transfert de l'énergie de résonance est le mécanisme primaire pour la migration de l'excitation électronique. Bien connu dans le contexte particulier de la photochimie moléculaire, c'est un phénomène dont la prévalence beaucoup plus grande tant dans les matériaux naturels que ceux de synthèse n'a été appréciée que lentement et pour laquelle la théorie fondamentale et sa compréhension ont fait des progrès importants au cours des dernières années. Avec la maturité croissante de bases théoriques solides, les derniers développements ont conduit à une identification complète des principes fondamentaux. Le présente revue décrit d'abord le contexte et les caractéristiques générales du transfert d'énergie avant de passer à une mise au point de ses caractéristiques électrodynamiques et photophysiques. On discute ensuite du rôle particulier que joue le mécanisme dans les matériaux photosynthétiques et les polymères synthétiques analogues et puis on résume ses applications principalement dans la détermination des structures biologiques. Enfin, on décrit plusieurs méthodes potentielles à l'aide desquelles il serait possible d'effectuer des commutations complètement optiques par le biais du contrôle et de l'application du transfert de l'énergie de résonance dans des nanostructures fabriquées d'une façon appropriée.

Mots-clés : « FRET », transfert d'énergie Förster, photophysique, fluorescence, laser.

[Traduit par la Rédactions]

1. Introduction

In a variety of complex materials, the close juxtaposition of basic units with suitable spectral character leads to a remarkable phenomenon: the absorption of light by one molecular species produces fluorescence unambiguously attributable to another. The effect is most readily apparent in chemical systems comprising two or more light-absorbing components (chromophores) with well-characterized absorption and fluorescence bands at broadly similar, but experimentally differentiable wavelengths. Observations of such phenomena illustrate the operation of a fundamental mechanism (the transfer of energy between molecules or chromophores) known as resonance energy transfer (RET) (1–3).[1] It is a mechanism that is found to operate across a chemically diverse and extensive range of systems, encompassing protein complexes, doped crystals, and solutions, to name but a few. Moreover, it also operates in systems where the end re-

Received 3 April 2008. Accepted 25 April 2008. Published on the NRC Research Press Website at canjchem.nrc.ca on 17 July 2008.

D.L. Andrews. School of Chemical Sciences, University of East Anglia, Norwich NR4 7TJ, United Kingdom (e-mail: d.l.andrews@uea.ac.uk).

[1]Also electronic energy transfer (EET); both terms are widely used.

 doi:10.1139/V08-099

Fig. 1. Typical spectral discrimination between the fluorescence from donor and acceptor species (here, notionally based on a cyan fluorescent protein donor and a yellow fluorescent protein acceptor): (*a*) the transmission characteristics of a short-wavelength filter ensure initial excitation of only the donor; a dichroic beam-splitter and another narrow emission filter ensuring that only the (Stokes-shifted) fluorescence from the donor reaches a detector; (*b*) in the same system, a longer-wavelength emission filter ensures capture of only the acceptor fluorescence, following RET.

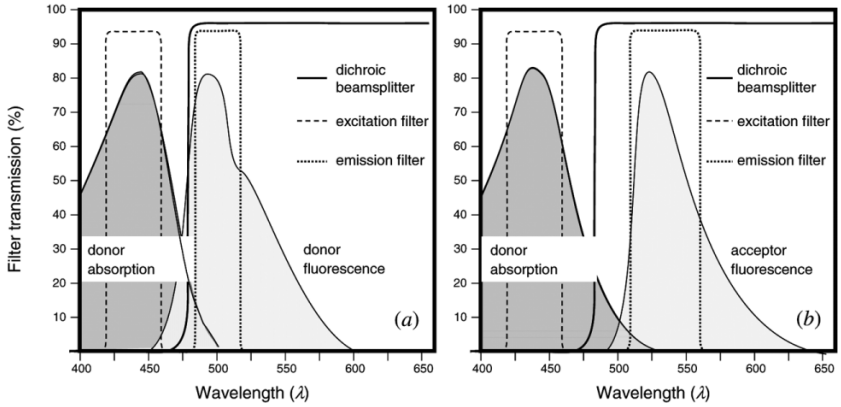

sult of optical absorption is not the release of energy in the form of fluorescence but optical frequency up-conversion or excitation capture in the form of chemical energy.

The singular properties of RET allow the flow of energy to exhibit a directed character (4–7). In complex multi-chromophore materials this effect contributes to a crucial, property-determining characteristic for the channeling of electronic excitation in photosynthetic systems (8), and the same principles are emulated in synthetic energy-harvesting systems such as the fractal polymers known as "dendrimers" (9). However, the observation and applications of RET extend well beyond the technology of light harvesting into numerous areas, several of which will be illustrated in later sections of this review. The phenomenon has an important function in the operation of organic light-emitting diodes (OLEDs) and luminescence detectors (10–14): in crystalline solids and glasses doped with transition metal ions, mechanisms based on RET are also engaged for laser frequency conversion (15–19). In the fields of optical communications and computation, a number of optical-switching and logic-gate devices are founded on the same principle (20–22). In the realm of molecular biology, the determination of protein structures and the characterization of dynamical processes is furthered by studies of the transfer of energy between intrinsic or "tag" chromophores (23–28); other ultra-sensitive molecular-imaging applications are again based on the same underlying principle (29–31). Further applications include the study of polymer interfaces (32), energy-transfer systems designed to act as sensitizers for photodynamic therapy (33), and as analyte-specific sensors (34–36).

The structure of the review is as follows: Section 2 describes the nature and general features of RET, focusing on its optical and photo-physical characteristics, and its uses in molecular structure determination: the underlying electromagnetic mechanism is addressed in more detail in Section 3. In Section 4, the particular role that energy transfer plays in photosynthetic materials and synthetic analogue polymers is discussed. Several possible methods are then described, in Section 5, for exerting optical control over RET, leading into a more general discussion of novel applications and nano-devices in the concluding Section 6.

2. Nature and characteristics of resonance energy transfer

To begin, it is appropriate to review the major features of RET. In this section, where the common attributes are first identified, "chromophore" is used as a generic term for the individual particles between which energy is exchanged. In crystalline, semi-crystalline, or glassy media, these centers of photon absorption (and subsequent energy release) may in fact take the form of ions, atoms, or colour centers; in other types of medium they may be small molecules, electronically distinct parts of large molecules, or nanoparticles, such as quantum dots. For their role in each transfer event, the participating chromophores in any such medium are designated "donor" and "acceptor", though it should be understood that any single chromophore acting in the capacity of acceptor for one transfer event may subsequently become the donor for a subsequent RET process.

A. Migration of electronic excitation in the condensed phase

When resonant ultraviolet or visible radiation impinges on any non-homogeneous dielectric material, the primary result of photon absorption is the population of electronic excited states in individual atomic, molecular, or other nanoscale centers. Typically, such absorption is followed immediately by a rapid but partial degradation of the acquired energy; the associated losses (largely due to vibrational dissipation) ultimately to be manifest in the form of heat. However, if any nearby chromophore has a suitably disposed electronic state, of a similar or slightly lower energy, that neighbour may acquire the major part of the electronic excitation through resonance energy transfer (a process that takes place well before thermal degradation of the excited state energy nears completion). The process is most commonly studied through spectrometric differentiation of fluorescence emerging from the initially excited energy donor and from the energy acceptor species, as illustrated in Fig. 1.

As will be shown in the following, the propensity for energy to be transferred between any two chromophores is severely restricted by distance, and if no suitable acceptor is

within reach, the donor will generally shed its energy by fluorescence or local dissipation. Conversely, any flow of energy that extends beyond conventional molecular dimensions will usually comprise a series of small-scale hops between near-neighbours. Pair interactions are therefore not only important in systems where the absorption of optical energy leads by direct transfer to the excitation of acceptor species; such interactions are also significant as representative components of the overall flow in complex, multichromophore systems. As such, it is appropriate to focus on the detailed character of these pair-transfer events.

B. Spectral overlap and the Förster equation

Though other possibilities exist, most transitions of donor decay and acceptor excitation are electric-dipole-allowed. Accordingly, the theory of pair transfer, beyond any region of wavefunction overlap, is traditionally based on electrodynamical coupling between transition dipoles. The first such formulation of the theory, which identified the inverse sixth power distance dependence (now often considered a hallmark of the transfer process) was made by Förster (37). Subsequently recast in quantum mechanical terms and experimentally verified by Latt et al. (38), this early theory of "radiationless" energy transfer remains widely applicable. Nonetheless, the Förster theory is subject to some conditions that were not originally appreciated, and it is not uncommon to find literature on the subject still perpetuating initial overstatements. Certain sources (see, for example, iupac.org) wrongly treat Förster "radiationless" energy transfer as exact, distinct, and separable from "radiative" energy transfer (the latter signifying successive but independent processes of fluorescence emission by a donor and capture of the ensuing photon by an acceptor). Although that certainly is the observed character of resonance energy transfer over relatively long distances, as for example between donor and acceptor components in a dilute solution, it is now known that both radiative and Förster transfer are simply the long- and short-range limits of one powerful, all-pervasive mechanism, as will be discussed in Section 3.

With this caution in mind, let us proceed to consider the pairwise transfer of excitation between two chromophores *A* and *B*. In the context of this elementary mechanism (potentially one RET component of a complex, multi-step migration process), *A* is designated the donor and *B* the acceptor. Specifically, let it be assumed that prior excitation of the donor generates an electronically excited species *A**. Forward progress of the energy is then accompanied by donor decay to the ground electronic state. Acquiring the energy, *B* undergoes a transition from its ground to its excited state. The complete RET process may be expressed by the following chemical equation:

$$[1] \qquad A^* + B \xrightarrow{\text{RET}} A + B^*$$

The excited acceptor, *B**, subsequently decays either in a further transfer event, or by another means, such as fluorescence. Because the *A** and *B** excited states are real, with measurable lifetimes, the core process of energy transfer itself is fundamentally separable from the initial electronic excitation of *A* and the eventual decay of *B*; the latter processes do not, therefore, enter into the theory of the pair transfer.

Fig. 2. Energetics and spectral overlap features (top) for energy transfer from *A* to *B* (and below, potentially backward transfer from *B* to *A*). For each chromophore, *F* denotes the fluorescence spectrum and σ the absorption. Wavy downward lines denote vibrational dissipation.

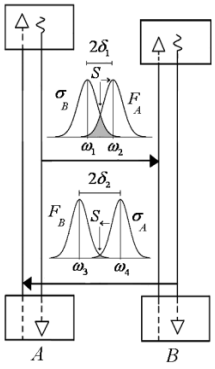

To delve more deeply into the nature of the process, it needs to be recognized that eq. [1] tells only part of the story, dealing as it does with only electronic excitations. In general, other dissipative processes are engaged (such features will be discussed in detail in later sections). In a solid, the linewidth of optical transitions manifests the influence of local electronic environments, which, in the case of strong coupling, may lead to the production of phonon sidebands. Similar effects in solutions or disordered solids represent inhomogeneous interactions with a solvent or host, while the broad bands exhibited by chromophores in complex molecular systems signify extensively overlapped vibrational levels, including those associated with skeletal modes of the superstructure. In each case, the level broadening allows pair transfer to occur at any energy level within the region of overlap between the donor emission and acceptor absorption bands, as illustrated in Fig. 2 (39).

For any donor–acceptor separation, *R*, substantially smaller than the wavelengths of visible radiation, the Förster theory gives the following expression for the rate of pairwise energy transfer w_F, for systems where the common host material for the donor and acceptor has refractive index *n*, at the optical frequency corresponding to the mean transferred energy (40):

$$[2] \qquad w_F = \frac{9\kappa^2 c^4}{8\pi\tau_{A^*} n^4 R^6} \int F_A(\omega)\sigma_B(\omega)\frac{d\omega}{\omega^4}$$

In this expression, $F_A(\omega)$ is the normalized fluorescence spectrum of the donor, τ_{A^*} is the associated radiative decay lifetime (related to the measured fluorescence lifetime τ_{fl} through the fluorescence quantum yield $\eta = \tau_{fl}/\tau_{A^*}$), $\sigma_B(\omega)$ is the linear absorption cross-section of the acceptor, ω is an optical frequency in radians per unit time, and *c* is the speed of light. The spectral functions F_A and σ_B are mathematically defined and discussed in detail in Section 3. As is evident from Fig. 2, the propensity for forward transfer is usually significantly greater than that for backward transfer owing to a sizeable difference in the spectral overlaps for the two processes. This feature, which is highly important in

Fig. 3. Relative orientations and positions of the donor and acceptor and their transition moments: (*a*) angles θ_A and θ_B subtended by donor and acceptor transition moments (not necessarily in the plane of the drawing) against the inter-chromophore displacement vector; (*b*) in-plane angle θ_T between the transition moments.

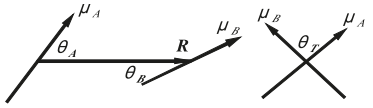

determining the efficiency of energy harvesting materials, is to be discussed in detail in Section 4.

The κ factor in [2] depends on the orientations of the donor and acceptor, both with respect to each other, and with respect to their mutual displacement unit vector $\hat{\boldsymbol{R}}$, as follows:

$$[3] \qquad \kappa = (\hat{\boldsymbol{\mu}}_A \cdot \hat{\boldsymbol{\mu}}_B) - 3(\hat{\boldsymbol{R}} \cdot \hat{\boldsymbol{\mu}}_A)(\hat{\boldsymbol{R}} \cdot \hat{\boldsymbol{\mu}}_B)$$

For each chromophore, $\hat{\boldsymbol{\mu}}$ designates a unit vector in the direction of the appropriate transition dipole moment (see Section 3). The possible values of κ^2, as featured in eq. [2], lie in the range (0, 4). It is evident that in the case of fixed chromophore positions and orientations, the result delivered by eq. [3] is a function of three independent angles as shown and defined in Fig. 3,

$$[4] \qquad \kappa = \cos\theta_T - 3\cos\theta_A \cos\theta_B$$

Unfavourable orientations can thus reduce the rate of energy transfer to zero; other configurations, including many of those found in nature, optimize the transfer rate. The angular disposition of chromophores is therefore a very important facet of energy transfer, and one that invites careful consideration in the design of light-harvesting materials. Note that transfer is not "necessarily" precluded when the transition moments lie in perpendicular directions (provided that neither is orthogonal to $\boldsymbol{R}$ (= $R\hat{\boldsymbol{R}}$)).

In any, at least partially, fluid or disordered system the relative orientation of all donor–acceptor pairs may not be identical, and it is then the distributional average of κ^2 that determines the overall measured response. In the isotropic case (completely uncorrelated orientations), the κ^2 factor averages to 2/3; departures from this value signify a degree of orientational correlation. In molecules of sufficiently high symmetry, it can also happen that either the donor or the acceptor transition moment is not unambiguously identifiable with a particular direction in the corresponding chromophore reference frame. Specifically, the electronic transition may then relate to a transition involving a degenerate state (as can occur with square-planar complexes, for example) (41). Alternatively, the same observational features might indicate rapid but orientationally confined motions. The considerable complication, which each of these effects brings into the trigonometric analysis of RET, has been extensively researched and reported by van der Meer (42).

C. Functional group separation and conformation diagnostics

One obvious field of applications for RET, based on its strong distance dependence, is the identification of motions in molecules, or parts of molecules, that can bring one chromophore into the proximity of another. There are many examples in biology, such as the molecular traffic across a cell membrane and protein folding (43–45). These and other similar processes can be registered by selectively exciting one chromophore using laser light and monitoring either the decrease in fluorescence from that species or the rise in the generally longer-wavelength fluorescence from the other chromophore as it adopts the role of acceptor. The judicious use of optical dichroic filters can make this fluorescence RET or "FRET" technique perfectly straightforward (see Fig. 1). In cases where the two material components of interest do not have suitable overlapped display absorption and fluorescence features in an appropriate wavelength range, molecular tagging with site-specific "extrinsic" (i.e., artificially attached) chromophores can solve the problem. Lanthanide ions, with their characteristically prominent and line-like absorption features, prove particularly useful in this connection (46).

In some applications, the actual distance between the chromophore groups is of specific interest. When the same two chromophores feature, in spatially different configurations, in the chemical composition of two different systems (again, a common feature in biology), then the relative displacements of the chromophores can be quantitatively assessed on the basis of comparisons between the corresponding RET efficiencies (23–28, 47). Such a technique is popularly known as a "spectroscopic ruler". Such elucidations of molecular structure usually lack information on the relative orientations of the groups involved, and as such, the calculations usually ignore the kappa parameter (see eq. [3]). The apparent crudeness of this approach becomes more defensible on realizing that even if it were to introduce a factor of two inaccuracy, the deduced group spacing would still be in error by only 12% (since $2^{1/6} = 1.12$). Refinements to the theory to accommodate the effect of fluctuations in position or orientation of the participant groups introduces considerable complexity, though progress is being made in several areas (48–50).

In experimental studies of RET, it is usually significant that the electronically excited donor can in principle release its energy by spontaneous decay, the ensuing fluorescence being amenable to detection by any suitably placed photodetector. Since the alternative possibility (that of energy being transferred to another chromophore within the system) has such a sharp decline in efficiency as the distance to the acceptor increases, it is commonplace to introduce the concept of a critical distance R_0 (a separation at which the theoretical rates of RET and spontaneous emission by the donor are equal, now known as the Förster distance). The Förster rate eq. is often cast in an alternative form, exactly equivalent to eq. [2], explicitly exhibiting this critical distance (51).

$$[5] \qquad w_F = \frac{3\kappa^2}{2}\frac{1}{\tau_{A^*}}\left(\frac{\overline{R}_0}{R}\right)^6$$

Here, $\overline{R}_0$ is defined as the Förster distance for which the orientation factor κ^2 assumes its isotropic average value, 2/3 (52). For complex systems the angular dependence is quite commonly disregarded, and the following, simpler expression employed

$$[6] \qquad w_F = \frac{1}{\tau_{A^*}}\left(\frac{R_0}{R}\right)^6$$

leading to a transfer efficiency Φ_T expressible as

$$[7] \qquad \Phi_T = \frac{1}{1+(R/R_0)^6}$$

Typical values of the Förster radius range over a few nanometers. Thus, when a given electronically excited chromophore is within a distance R_0 of a suitable acceptor, RET will generally be the dominant decay mechanism; conversely, for distances beyond R_0, spontaneous decay will be the primary means of donor deactivation.

Before continuing, it is nonetheless worth observing that other forms of coupling are also possible, although less relevant to most systems of interest in the following account. For example, the transfer of energy between particles or units with significantly overlapped wavefunctions is usually described in terms of Dexter theory (53), where the coupling carries an exponential decay with distance, directly reflecting the radial form of overlapping wavefunctions and electron distributions. Compared to materials in which the donor and acceptor orbitals do not spatially overlap, such systems are of less use for either device or analytical applications largely because the coupled chromophores lose their electronic and optical integrity. This is the main reason why complex light-harvesting systems are commonly designed with "non-conjugated" linkages or spacer units between the chromophores, or else with the latter held on a host superstructure preventing direct chromophore contact. Parallels can be drawn with the way a dielectric layer operates in a simple electrical capacitor. In the alternative scenario, where spacer units act as a "conductive" bridge through delocalization and mixing of their orbitals with the donor or acceptor orbitals, energy transfer is specifically expedited by the operation of a special "superexchange" mechanism (54, 55), which, despite efficiency gains, compromises diagnostic applications.

D. Decay kinetics and polarization features

When linearly polarized laser light is used to excite any specific species within a complex disordered solid or liquid system, the probability for excitation of any particular molecule is proportional to $\cos^2\theta$, where θ is the angle between the appropriate excitation transition moment and the electric polarization vector of the input radiation. Consequently, the population of excited molecules has a markedly anisotropic distribution, a phenomenon associated with the term "photoselection". If radiative decay were to ensue instantaneously, i.e., from precisely the same excited level, then the fluorescence would carry the full imprint of that anisotropy and itself exhibit a degree of polarization (the highest value possible). Accounting for the necessary three-dimensional rotational average (56), it is readily shown that the fluorescence intensity components polarized parallel to and perpendicular to the polarization of the excitation beam, $I_\parallel$ and $I_\perp$ respectively, would then lie in the ratio 3:1. Commonly observed departures from this result thus signify the extent to which the orientation of the emission dipole differs from that of the prior, initial excitation, which may be due to intervening decay, molecular motion, or intermolecular energy transfer. The two most widely used quantitative expressions of this effect are the "fluorescence anisotropy", r, or the "degree of polarization", P, defined and related as follows

$$[8] \qquad r = \frac{I_\parallel - I_\perp}{I_\parallel + 2I_\perp}, \qquad P = \frac{I_\parallel - I_\perp}{I_\parallel + I_\perp} \quad \Rightarrow \quad r = \frac{2P}{3-P}$$

When the donor and acceptor have transition dipole moments oriented in parallel, then $r = 0.4$ and $P = 0.5$.

The key factor determining any loss in polarization is the angle θ between the directions of the absorption and emission transition dipole moments. In terms of this indicator, the case where internal decay intervenes between excitation and fluorescence decay, within a single molecule, is no different from that of a donor–acceptor pair where the absorption and emission processes are spatially separated (provided the donor and acceptor have a fixed mutual orientation, and the orientation of the pair is random). The following result, derived by Levshin (57) and Perrin (58), can be applied in both cases

$$[9] \qquad P = \frac{3\cos^2\theta - 1}{3 + \cos^2\theta}$$

In the case of a donor–acceptor pair, θ is to be interpreted as the angle θ_T shown in Fig. 3. Equation [9] thus allows direct calculation of this microscopic parameter through measurement of the macroscopic quantity P. Moreover, when P proves to exhibit a time-dependent decay, a study of the kinetics provides information on the extent of rotational motion intervening between the absorption and emission events.

Very different behaviour is observed for RET systems in which the donor and acceptor are orientationally uncorrelated, i.e., where they are both, independently, randomly oriented. In such cases, there is a very rapid loss of polarization "memory", and it transpires that the associated degree of anisotropy is precisely 1/25, i.e., $r = 0.04$ (1); two or more energy-transfer jumps will therefore usually, to all intents and purposes, totally destroy any polarization in any ensuing fluorescence. However, it should be noted that there is a surprising recovery in the anisotropy at distances approaching the transfer wavelength, as will be shown in Section 3C. The effect is sufficiently strong to warrant attention in dilute solution studies.

3. Electromagnetic mechanism

In each area of application, RET measurements exploit key features that originate in the detailed electromagnetic origins of RET coupling. To elicit these features, it is necessary to look more closely at the fundamental nature of the interactions involved.

A. Transition dipole coupling

The spectral functions featured in eq. [2] can be expressed in terms of the electronic transition properties of the chromophores, taking into account their vibrational structure. Although each transition spans a range of frequencies within the overall spectral bandwidth, it can be assumed under the conditions of the Born–Oppenheimer approximation that the vibrational factors in the transition dipole moments

factor out as Franck–Condon factors. The mathematical definitions of $F_A(\omega)$ and $\sigma_B(\omega)$ are then expressible as follows, using Dirac notation

$$[10] \quad F_A(\omega) = \frac{\omega^3 \tau_{A*} \mu_A^2}{3\varepsilon_0 \pi c^3} \sum_{n,r} \rho_{A*}^{(n)} \left| \left\langle \varphi_A^{(r)} \middle| \varphi_{A*}^{(n)} \right\rangle \right|^2 \delta(E_{A_n^*} - E_{A_r} - \hbar\omega)$$

$$[11] \quad \sigma_B(\omega) = \frac{\pi\omega \mu_B^2}{3\varepsilon_0 c} \sum_{m,p} \rho_B^{(m)} \left| \left\langle \varphi_{B*}^{(p)} \middle| \varphi_B^{(m)} \right\rangle \right|^2 \delta(E_{B_p^*} - E_{B_m} - \hbar\omega)$$

Here, μ_A and μ_B are the transition electric dipole moments for the donor decay and acceptor excitation, specifically given by

$$[12] \quad \boldsymbol{\mu}_A = \left\langle \psi_A \middle| \boldsymbol{\mu} \middle| \psi_{A*} \right\rangle, \quad \boldsymbol{\mu}_B = \left\langle \psi_{B*} \middle| \boldsymbol{\mu} \middle| \psi_B \right\rangle$$

where the μ is the dipole operator and each ψ is an electronic-state wavefunction. The indices *m*, *n*, *p*, and *r* in eq. [11] are generic labels denoting vibrational sub-levels, with each φ representing an associated wavefunction and *E* the corresponding energy; ρ denotes a population distribution function for the initial state of each species. Comparing the above results with eqs. [2] and [3] reveals the intrinsic quadratic dependence of the energy transfer rate on a coupling of the form

$$[13] \quad C = \frac{\left|\boldsymbol{\mu}_A\right| \left|\boldsymbol{\mu}_B\right|}{4\pi\varepsilon_0 R^3} [(\hat{\boldsymbol{\mu}}_A \cdot \hat{\boldsymbol{\mu}}_B) - 3(\hat{\boldsymbol{R}} \cdot \hat{\boldsymbol{\mu}}_A)(\hat{\boldsymbol{R}} \cdot \hat{\boldsymbol{\mu}}_B)$$

isomorphous with the usual formula for the interaction of two static dipoles. However, the result given by eq. [13] is an off-diagonal quantum amplitude connecting different initial and final states (only a diagonal quantum amplitude can directly signify energy). This is one of several important distinctions, the significance of which becomes more apparent when the quantum electrodynamical theory is developed.

Before continuing, it is worth emphasizing that the familiar inverse sixth power distance dependence of RET rate in the short range specifically owes its origin to the quadratic rate dependence on a coupling of transition electric *dipoles*. The result is, of course, applicable only when both the donor-decay and acceptor-excitation transitions are electric dipole (*E*1) allowed. In general, the coupling is effected by the lowest orders of multipole, electric or magnetic, that can support the necessary donor and acceptor transitions. In the Förster range, the distance dependence exhibits the form $R^{-(P+Q+1)}$ for the coupling of two transition electric multipoles *EP-EQ*, or two magnetic multipoles *MP-MQ*; whilst for the coupling of an electric with a magnetic multipole, *EP-MQ*, the distance dependence is $R^{-(P+Q)}$ (59, 60). For example, the coupling of an electric dipole decay with an electric quadrupole excitation, *E*1-*E*2, has an R^{-4} distance dependence within the Förster range. However, it should be borne in mind that each unit increase in multipolar order and each substitution of an electric transition by a magnetic counterpart lowers the strength of the coupling by a factor of two to three orders of magnitude. The decreasing efficiency of successive multipole orders increasingly disfavours the role of RET in the decay of the donor, compared with other decay mechanisms.

B. Near-field and long-range behaviour

As mentioned above, Förster theory is subject to several limitations. It is a theory specifically applicable under near-field conditions, i.e., over donor–acceptor distances significantly less than the optical wavelength for the energy being transferred, and this is a constraint that is effective for the coupling between any order of multipolar transitions. This condition is not always satisfied; however, there are numerous systems in which typical donor–acceptor distances approach or even exceed such wavelengths. Under those circumstances, new "retardation" features emerge, reflecting the finite time for the propagation of energy between molecular sites.

To ascertain rate expressions that correctly represent both short- and long-range transfer requires a fundamentally rigorous, quantum mechanical basis that delivers properly retarded solutions. The most suitable framework is afforded by quantum electrodynamics (QED) (61, 62) whose wider successes, such as its correct predictions of the magnetic moment of the electron, the Lamb shift, and the Casimir effect, are well-known (63). Less well-known is the fact that QED alone provides a satisfactory mechanistic explanation for the much more familiar process of spontaneous emission, or that even the use of electric and magnetic multipoles is ultimately defensible only in the context of a fully quantum electrodynamical theory (64). In connection with the theory of resonance energy transfer, the development of a theory based on QED began in pioneering work by Avery, Gomberoff, and Power (65, 66), culminating in a unified theory (67) whose ramifications continue to be explored today (68). A concise exposition is presented below.

A suitable starting point is the following Hamiltonian, for the simple RET system comprising chromophores A and B

$$[14] \quad H = H_A + H_B + H_{int}(A) + H_{int}(B) + H_{rad}$$

Here, the first two terms are the unperturbed Hamiltonian operators for the chromophores, and the two H_{int} operators represent interactions of the radiation field with A and B. The final term, H_{rad}, is the radiation Hamiltonian, which, as befits an operator, is always part of the sum even when there are no photons present. No term in eq. [14] directly links A with B, in other words, there is no static or "longitudinal" coupling; any form of coupling between the two chromophores can only be mediated by their individual interactions with the radiation field. This is an exact feature of any development in terms of multipole transitions (true not only for electric dipole interactions but for every other order of electric and magnetic multipole).

In the electric-dipole approximation, each $H_{int}(\xi)$ is given by the usual dipole coupling formula

$$[15] \quad H_{int}(\xi) = -\sum_{\xi} \boldsymbol{\mu}(\xi) \cdot \boldsymbol{e}^{\perp}(\boldsymbol{R}_{\xi})$$

where the electric-dipole moment operator, $\mu(\xi)$, operates on matter states, and the transverse electric field operator, $\boldsymbol{e}^{\perp}(\boldsymbol{R}_{\xi})$ on electromagnetic radiation states; $\boldsymbol{R}_{\xi}$ is the position vector of the chromophore labeled ξ. By standard methods, the electric field operator can be cast in the form of a summation over optical modes, each mode characterized by wavevector and polarization. Every operation of H_{int} is then asso-

ciated with the creation or annihilation of a photon from one of these modes. Throughout the usual pairwise process of RET, there is no applied radiation involved (the initial photoexcitation and any fluorescence being physically separable events); hence, the lowest order process that can couple the donor-decay and acceptor-excitation transitions is one involving the creation and annihilation of a "virtual" photon. Such photons are not physically observed; the quantum theory accordingly requires a sum to be taken over all radiation modes (i.e., all possible wave-vectors and polarizations). Since $H_{\rm int}$ must feature twice (once to create the virtual photon and the second time to annihilate it), the quantum amplitude $M_{\rm fi}$ for RET is determined by second-order perturbation theory

$$[16] \qquad M_{\rm fi} = \sum_r \frac{\langle f|H_{\rm int}|r\rangle\langle r|H_{\rm int}|i\rangle}{(E_i - E_r)}$$

where i, f, and r denote initial, final, and intermediate states of the system, respectively, and E signifies an energy. Two possible interaction sequences arise: (*a*) the virtual photon is created at A (effecting the decay of the donor excited state) and subsequently annihilated at B (effecting the acceptor excitation); (*b*) the virtual photon is created at B (along with the acceptor excitation) and annihilated at B (with the donor decay). These two possibilities are both represented within a state-sequence diagram as shown in Fig. 4. The counter-intuitive nature of case (*b*) does not preclude its inclusion in the calculation; it can be understood that exact energy conservation is not imposed during the interval between creation and annihilation of the virtual photon, i.e., the ultrashort photon flight-time. This, a key feature of virtual photon behaviour, is consistent with the time-energy Uncertainty Principle. When the whole system enters its final state, the balance of energy conservation is once again restored.

The explicit evaluation of eq. [16] by any of several standard techniques requires a considerable amount of algebra and calculus; details can be found in the original papers and subsequent reviews (69, 70). The result emerges in a form concisely expressible as follows

$$[17] \qquad M_{\rm fi} = \mu_{{\rm A}i} V_{ij}(k,\boldsymbol{R}) \mu_{{\rm B}j}$$

where the subscript indices i and j stand for Cartesian components, and the convention of summation over repeated indices is implicit. The value of k is $2\pi/\lambda$, where λ is the wavelength associated with the transfer energy. In eq. [17], the two transition dipole moments, for the donor-decay and acceptor-excitation transitions, are coupled by an $E1 - E1$ coupling tensor defined by

$$[18] \qquad V_{ij}(k,\boldsymbol{R}) = \frac{e^{ikR}}{4\pi\varepsilon_0 R^3}\{(\delta_{ij} - 3\hat{R}_i\hat{R}_j) - (ikR)(\delta_{ij} - 3\hat{R}_i\hat{R}_j) - (kR)^2(\delta_{ij} - \hat{R}_i\hat{R}_j)\}$$

Before considering the rate equation that ensues from the above QED treatment, some features of physical significance can be identified directly from the quantum amplitude. First,

Fig. 4. State-sequence diagram for RET, progressing from the initial system state of the left, through intermediate states, to the final state on the right. In each box, the two circles designate the states of *A* and *B*, black indicating the ground state; ϕ denotes a virtual photon. The lower route (*a*) and the upper route (*b*) signify the two quantum pathways.]

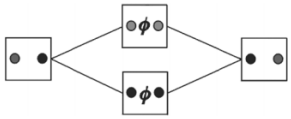

it is important to note that for short-range distances where $k\boldsymbol{R} << 1$ (signifying a length significantly smaller than the wavelength of the donor decay), eq. [18] couples with the transition dipoles in [17] to deliver a result that equates exactly with the classical expression for the coupling, eq. [13]. The additional terms in [18], identified by QED, come into play at larger distances (signifying the accommodation of retardation principles). These are features that reflect the finite interval over which the energy exchange between A and B can be accomplished which is restricted by the photon propagation time, in accordance with relativistic causality.[2]

To appreciate the range-dependent character of the RET rate on its own merits, let it be assumed for simplicity that the donor and acceptor have isotropically averaged orientations, and that the refractive index of the medium is unity. It then follows that the distance-dependence of the transfer rate factorizes out in the following form (67, 71) (one that also identifies it with the tensor inner product of the coupling tensor in eq. [18]).

$$[19] \qquad \langle A(k,R)\rangle = \frac{1}{8\pi^2\varepsilon_0^2 R^6}\{3 + (kR)^2 + (kR)^4\} = V_{ij}(k,\boldsymbol{R})\overline{V}_{ij}(k,\boldsymbol{R})$$

This orientationally averaged transfer function is a scalar characterizing the distance dependence of $E1$-$E1$ coupling in RET. A key property of the result is that as the distance R increases into the range where it substantially exceeds the wavelength for the transfer energy, i.e., where $k\boldsymbol{R} >> 1$, the third term in eq. [19] begins to dominate, and the overall dependence on R assumes an inverse-square form. Detailed calculations reveal that the limiting result tallies exactly with radiative emission by the donor, followed by acceptor absorption of the ensuing radiation. In other words, the photons involved in the energy transfer lose their virtual character and become real, as is consistent with their acquiring a finite (and in principle measurable) time of flight. This change in character of RET with distance is neatly illustrated by a plot of the isotropically averaged excitation transfer function, as shown in Fig. 5. This figure gives a readily comprehensible representation of the Förster radiationless and radiative transfer processes as short- and long-range asymptotes, respectively, shown by the change in gradient of the log–log plot between the short- and long-range regions.

The discovery that Förster radiationless and radiative coupling are components of a single mechanism that operates seamlessly over *all* distances beyond wavefunction overlap

[2] Equally when $k = 0$ (essentially the transfer of an infinitesimal energy with infinitely long wavelength) the result (see eq. [18]) reduces to a form in which the near-field term alone operates out to infinity, duly corresponding to a coupling of "static" dipoles.

Fig. 5. Log–log plot of the RET excitation transfer function $\langle A(k,R)\rangle$, as defined by eq. [19], against log R (in meters), for $k = 9 \times 10^6$ m^{-1} (corresponding to a wavelength at the red end of the visible region). The dotted line shows the radiative asymptote (slope –2).

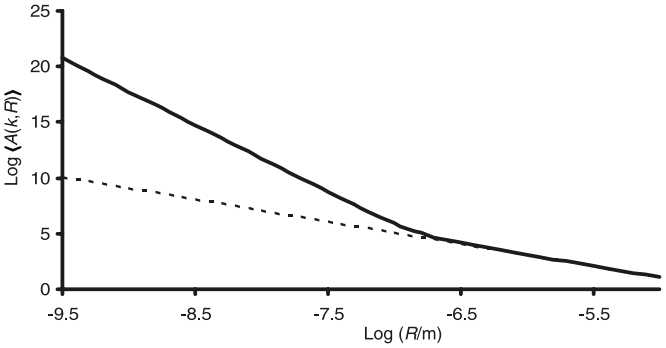

resulted in a paradigm shift in the understanding of RET, and it is the reason why the QED theory has been termed a "unified" theory (67). This theory is valid over a span ranging from the nanoscale up to indefinitely large distances; Förster energy transfer is the short-range asymptote and radiative transfer the long-range asymptote. One consequence of this discovery is that it has become meaningless to entertain any notion of competition between these processes. Recently, a revisitation of the QED theory has enabled the individual contributions associated with each of the two quantum pathways to be disentangled (72), proving that the long-range R^{-2} behaviour is completely identifiable with the physically more intuitive sense of propagation, the lower pathway in Fig. 4. In the same regime, the contribution from the upper pathway unexpectedly drops off as R^{-8}. Nonetheless in the near-zone, both run as R^{-6}. However, it should be emphasized that the unified theory establishes more than this; it also addresses donor–acceptor separations in an intermediate range where neither the radiative nor the Förster mechanism is truly valid. An experimental verification of the behaviour in this region remains a currently unfulfilled objective, a point we shall return to shortly.

The majority of applications of RET relate to the Förster regime, i.e., they involve systems in which stepwise energy transfer events occur between chromophores separated by less than the Förster distance, and as such they are also usually operating within the short-range, $k\boldsymbol{R} << 1$. Systems in which the mean transfer distance might fall in the long-range regime, $k\boldsymbol{R} >> 1$, would necessarily require the optically relevant species to be present in low concentrations; moreover, any diffusion processes that could produce transient short-range donor–acceptor juxtapositions should also have a timescale significantly longer than the donor decay time, or else diffusion-limited Förster transfer would result. The radiative transport that ensues in the latter case is exhibited in a variety of systems, such as dilute dye solutions, and it leads into a distinct branch of the theory where multiple scattering must also be taken into account. A detailed account is given by Berberan-Santos et al. (73).

C. Orientational and refractive effects

It is not only the effective power law governing distance that changes form as donors and acceptors move further apart, but also their functional dependence on orientation changes. To fully describe this feature, it is expedient to introduce the following generalization of the κ factor earlier defined by eq. [4]

Fig. 6. Variation with distance of the fluorescence anisotropy following RET between freely and independently rotating (or randomly oriented) donor and acceptor chromophores. Plot shows the acceptor fluorescence anisotropy r as a function of distance, represented on the abscissa scale as values of kR.

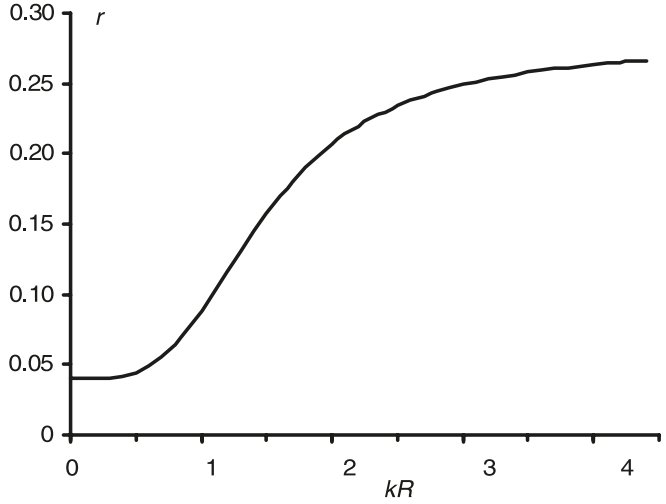

$$[20] \qquad \kappa_n = \cos\theta_T - n\cos\theta_A\cos\theta_B$$

Then, it can be shown that the excitation transfer function, whose isotropic average was given as eq. [19], more generally takes the form

$$[21] \qquad A(k,R) = \frac{9}{16\pi^2\varepsilon_0^2 R^6}\{\kappa_3^2 + (\kappa_3^2 - 2\kappa_1\kappa_3)(kR)^2 + \kappa_1^2(kR)^4\}$$

Equation [21] applies in the case of chromophores that are fixed, or have limited orientational freedom. Although most configurations will exhibit a variation in their orientational dependence with any significant change in donor–acceptor separation, it is the case that when $\mu_A \perp \mu_B$ and one of these transition dipoles is also orthogonal to $\boldsymbol{R}$, RET is entirely dipole forbidden "at all" distances. It is also notable that, although different kappa factors characterize the terms in R^{-6}, R^{-4}, and R^{-2}, both κ_3 and κ_1 feature in the expression for R^{-4}. This is the main reason why the intermediate term has eluded experimental identification, because it is technically difficult to envisage any circumstances in which its contribution could be isolated.

An interesting interplay of distance and orientational factors does however arise in connection with fluorescence polarization measurements, and this might afford the best means of identifying the onset of retardation effects. Calculations show that the fluorescence anisotropy in a system of freely and independently rotating donors and acceptors dramatically increases from its usual value $r = 0.04$, for transfer distances beyond the usual near-zone. The result, shown in Fig. 6, exhibits a long-range asymptote of precisely $r = 0.28$ (74). The reason for this behaviour is best understood as reflecting a "decreased" anisotropy in the short range (where

the transfer is effected by a photon whose virtual character means its propagation is not specifically aligned to the interchromophore direction) (69). Consequently its communication of polarization information is also less precise than is the case for the increasingly real-character photons that become involved in propagation over larger distances. Significant though the result is, its interpretation in any solution study would be significantly complicated by the need to accommodate an ensemble distribution of transfer distances.

To finally secure a completely general and rigorous result for RET requires that due consideration be given to the electronic influence of other material in the vicinity of the donor and acceptor. For optically dense systems, such matter could comprise other potential donor or acceptor species; in doped solids, it would be the host crystal that exerts the primary electronic influence; in the case of solutions, the surroundings would mostly comprise solvent, whereas in photobiological materials, it would usually be a protein superstructure and solvation, for example. Scholes et al. have recently performed extensive quantum chemical calculations quantifying such effects in a host of photosynthetic light-harvesting systems (75, 76).

A more comprehensive and general representation of media effects in each of these systems can be secured from the premise that the bulk material exerts an influence over resonance energy transfer by its effect on real or virtual photon propagation. The detailed form of this influence is duly accommodated in the theory by the introduction of an effective radiation field operator whose eigenstates signify modes in which photons are "dressed" by the electromagnetic influence of the host (77). Strictly, these dressed photons are "polaritons", though the distinction is not important if one is dealing with frequencies at which the host is relatively transparent. By a lengthy development, it transpires that the effect of making this correction is for the coupling tensor in eq. [18] to emerge in the following modified form, assuming Lorentz local field factors are assimilated into the expressions for the spectral functions $F_A(\omega)$ and $\sigma_B(\omega)$.

$$[22]\quad V_{ij}(k,\boldsymbol{R}) = \frac{1}{n^2(\omega)}\frac{e^{in(\omega)kR}}{4\pi\varepsilon_0 R^3}\{(\delta_{ij}-3\hat{R}_i\hat{R}_j) - (in(\omega)kR)(\delta_{ij}-3\hat{R}_i\hat{R}_j) - (n(\omega)kR)^2(\delta_{ij}-\hat{R}_i\hat{R}_j)\}$$

Here, $n(\omega)$ is the complex refractive index for optical frequency $\omega = ck$. The imaginary part of this index leads, through its inclusion in the phase factor in eq. [22], to dissipative losses, which properly increase with distance.

In its final and most general form, consistent with eqs. [21] and [22], it emerges that the RET rate can be written as follows (78)

$$[23]\quad w = w_F + w_I + w_{rad}$$

$$[24]\quad \left.\begin{aligned} w_F &= \frac{9\kappa_3^2 c^4}{8\pi\tau_{A^*}R^6}\int F_A(\omega)\sigma_B(\omega)\frac{d\omega}{\omega^4 n^4(\omega)} \\ w_I &= \frac{9c^2}{8\pi\tau_{A^*}R^4}(\kappa_3^2-2\kappa_i\kappa_3)\int F_A(\omega)\sigma_B(\omega)\frac{d\omega}{\omega^2 n^2(\omega)} \\ w_{rad} &= \frac{9\kappa_i^2}{8\pi\tau_{A^*}R^2}\int F_A(\omega)\sigma_B(\omega)\,d\omega \end{aligned}\right\}$$

The first term of eq. [24] is the usual Förster rate, identical to eq. [1] if the refractive index is taken as a constant. The second contribution, w_I, is a correction that comes into play at distances beyond the near-field, where the assumption $k\boldsymbol{R} << 1$ no longer holds. The third term, w_{rad}, which dominates over both other contributions when $k\boldsymbol{R} >> 1$, equates to radiative transfer. For donor–acceptor distances in the hundreds of nanometers range, where $k\boldsymbol{R} \approx 1$ to the nearest order of magnitude, all three terms of eq. [24] significantly contribute to resonance energy transfer.

4. Role in energy-harvesting materials

A. Optical energy collection and directed transfer

Many of the most widely studied and well-characterized theatres of operation for RET are to be found in connection with light-harvesting materials (both naturally occurring biological systems and synthetic structures). Following the capture of a photon by any such system, the transfer mechanism dictates that the migration of the acquired energy from the site of the initial photoabsorption through to the site of its utilization is at every stage subject to an inverse sixth-power dependence on distance. As a result, energy migration over distances beyond the Förster radius mostly operates through a series of short hops rather than one long one. Moreover, a "spectroscopic gradient" is commonly associated with these hops (79), the term signifying progressively longer wavelengths for absorption and fluorescence in successively visited chromophores (recall Section 2B). This property contributes significantly to the high efficiency of photosynthetic and allied energy-harvesting systems.

In considering the effectiveness of a preferred direction to the traffic between any two chromophores involved in such a sequence of energy transfer steps, it will be immediately apparent that there is a close similarity of form between the eqs. for "forward" and "backward" transfer between any given pair of electronic levels. The distance aspects for forward and backward transfer are obviously the same; moreover, since the unit displacement vector becomes $-\hat{\boldsymbol{R}}$ for back-transfer, its quadratic involvement in the orientation factor κ^2 means the latter is also identical. By reference to eqs. [10] and [11], and considering their counterparts for the inverse transfer process, it is in fact clear that the key to imposing directedness principally lies in exploiting differences in the relative spectral profiles. To quantify the relative rates or propensities for forward and backward transfer, it has been found convenient to introduce a dimensionless relative directional efficiency, ε, defined by

$$[25]\quad \varepsilon = \frac{\tau_B\int F_A(\omega)\sigma_B(\omega)\omega^{-4}d\omega}{\tau_A\int F_B(\omega)\sigma_A(\omega)\omega^{-4}d\omega}$$

The spectral curves illustrated in Fig. 2 exhibit typical implications for the spectral overlaps in the numerator and denominator of eq. [25]. For each chromophore, the fluorescence peak is Stokes-shifted to a lower frequency with respect to its absorption counterpart. Moreover, in the majority of cases of interest the peak of the acceptor absorption curve lies at a lower frequency than that of the donor emission. Thus, it becomes clear that forward transfer in any one step is generally favoured because (with reference to the

parameters shown in Fig. 2) $\omega_4 - \omega_3 > \omega_2 - \omega_1$, signifying that δ_2 will exceed δ_1.

In a recent study accommodating both symmetric and asymmetric lineshapes, detailed analytical results have been determined for the directional efficiency ε (39). In the case of Gaussian spectra, a particularly simple result applies if the two species possess similar fluorescence lifetimes, and if their absorption and fluorescence curves have similar heights and full-widths at half maximum, ω_{FWHM}. Under these conditions, the following result emerges

$$[26] \quad \varepsilon \cong e^{2k(\delta_2^2 - \delta_1^2)}$$

where $k = (4 \ln 2)\omega_{FWHM}^{-2}$. Equation [26] exhibits a transfer efficiency that strongly increases with δ_2 and decreases with δ_1, as might qualitatively be anticipated. Furthermore, if the Stokes shifts for A and B are equivalent and represented by $\omega_S = \omega_4 - \omega_2 = \omega_1 - \omega_3 = \delta_2 - \delta_1$, and the shift characterizing the spectroscopic gradient is defined as $\omega_G = \omega_4 - \omega_1 = \omega_2 - \omega_3 = \delta_1 + \delta_2$, then the directional efficiency is expressible in its simplest form

$$[27] \quad \varepsilon = e^{2k\omega_G\omega_S}$$

It is notable that this result shows the same functional dependence on the spectroscopic gradient and the Stokes shift; both are equally important in determining the directedness of the energy transfer. In an energy-harvesting system consisting of a number of chemically or environmentally different fluorophores, a progressive spectroscopic gradient operating at every energy transfer step thus ensures an overall directionality of flow, a characteristic summarized in the term "energy funnel".

B. Excitons and excitation pooling in photosynthetic systems

To achieve their primary purpose in green plants, leaf structures contain numerous copies of the complex molecular apparatus for synthesizing sugars from carbon dioxide and water. Further to these photosynthetic reaction centres, simpler and more numerous antenna pigments are additionally required to absorb incident light. However, many other structural elements have also to be present; crucially, there must be components that deliver H_2O, CO_2, and photoexcitation energy to the reaction centres, and still others to take the sugars off to where they are required as building materials for new plant tissue. To optimize the overall photosynthetic efficiency of the organism, a trade-off is therefore necessary between the density and arrangements of pigments and reaction centres. Such organizational criteria are further complicated by a consequence of simple chemical energetics; the fact that several visible photon energies are required to effect the synthesis of each carbohydrate unit. Photosynthesis thus also requires a gathering of the necessary energy into one location.

To most effectively utilize the sunlight that falls upon them, photosynthetic organisms typically have a system of antenna complexes surrounding the reaction centers where photosynthesis takes place (80–83). The antenna complexes absorb light, and the acquired energy is transferred onwards through a series of short-range, radiationless energy-transfer steps as illustrated in Fig. 7. Specific channelling to the reaction centres is cleverly accomplished by connectivity between spectroscopic and kinetic features, i.e., a correlation of the spatial locations of the chromophores with a progressive spectroscopic gradient. In the overall migration of energy from the site of its initial deposition to the site of its chemical action, this directionality obviates what would otherwise be random diffusion; on the contrary, it means that energy is quickly and efficiently directed to the site of its chemical utilization. Not only does this allow an organism to harvest light incident on a large surface area but also by pooling energy from a large number of antenna chromophores, energy of a higher equivalent frequency can be produced.

Fig. 7. Schematic energy flow in a bacterial photosystem for the oxidation of water.

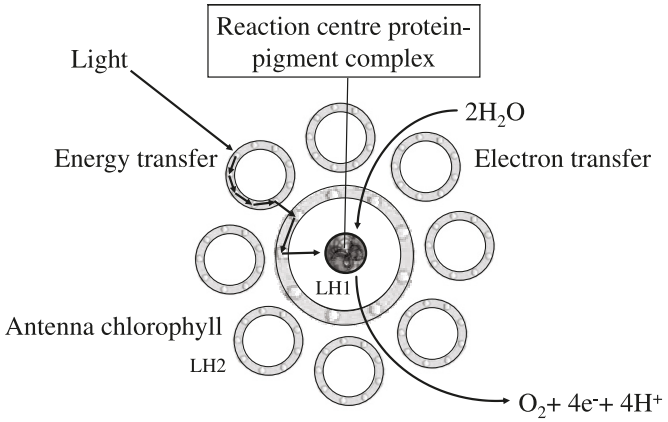

Not only the spectroscopic properties of the chromophores determine the character and direction of energy flow, but the chromophore positioning and orientation are also important. Two-dimensional optical spectroscopy can unveil the intricate interplay between spectral and spatial overlap features in light-harvesting complexes, as beautifully exhibited in a recent study on bacteriochlorophyll (84). Interrogating the system with a sequence of ultrashort laser pulses, the optical response reveals linear absorption processes as well as couplings between the chromophores and dynamical aspects of the energy transfer. The results show that excitation relocation does not simply proceed by stepwise transfer from one energy state to another of nearest energy, but it depends on strong coupling between chromophores (as determined by the extent of their spatial overlap), further limiting any residual randomness in direction of the energy transfer. In other studies on photosynthetic systems, it has also emerged that energy transfer can propagate with a wave-like motion due to quantum coherence (85).

Fluorescence polarization measurements are a powerful means of eliciting other structural information. Because photosynthetic systems are relatively rigid systems with chromophores held at fixed positions and orientations relative to each other, then even when there are several successive energy jumps, any resulting emitted fluorescence is generally polarized. The extent of this polarization affords invaluable information about the internal orientational structure, as was outlined in Section 2D.

C. Energy-harvesting dendrimers

The proven efficiency of photosynthetic units and the elucidation of the responsible mechanisms have stimulated the

design of a variety of synthetic light-harvesting systems (86–88). The materials that have received most attention are dendrimers (89–92) (macromolecules consisting of molecular units repeatedly branching out from a central core designed to act as an excitation trap, exemplified by the structure in Fig. 8).

The outward branching leads to successive generations of structures, each with an increased number of peripheral antenna chromophores. In ideal cases, the requisite spectroscopic gradient is established through chemically similar chromophores in generationally different locations (93, 94). Most recent work on dendrimers has utilized branching motifs of vertex degree three and four, based on tri-substituted benzene (90) and porphyrin rings (95), respectively.

Modelling the multi-step flow of energy in dendrimers presents a considerable challenge (96, 97), and a variety of calculational methods have been brought to bear on the problem. Often, simplifying assumptions are required; for example, in work by Blumen et al. (98) an exact solution has been derived for fractal polymers in which all chromophores have the same absorption cross-section and all rates of transfer between nearest neighbours are considered equal. More radical approaches to the problem have also been attempted, such as modeling the diffusion of the excitation under a constant force as a continuum process (99), or using the Eyring (membrane permeation) model to treat the energy flux as diffusion in a potential energy landscape with thermal barriers (100).

One recently developed method that shows promise is an operator approach developed from an "adjacency matrix" representation, based on the chemical connectivity between individual chromophores (101–103). Here, a square matrix, whose order equals the number of chromophores, represents the propensities (probabilities associated with a specific time interval) for energy migration between the chromophores. This matrix operates upon a vector representation of the population conditions, each iteration representing an advance in time. Considerable simplification is effected, without compromising the fidelity of the model, by collapsing the representation into a reduced basis whose order is generational number of the dendrimer. For a three-generation dendrimer, for example, the RET propensity matrix in the shell basis may be written as follows

$$[28] \qquad \tilde{\mathbf{C}} = \begin{pmatrix} 1-a_3 & 2\varepsilon_3^{-1}a_3 & 0 & 0 \\ a_3 & 1-a_2-2\varepsilon_3^{-1}a_3 & 2\varepsilon_2^{-1}a_2 & 0 \\ 0 & a_2 & 1-a_1-2\varepsilon_2^{-1}a_2 & 3\varepsilon_1^{-1}a_1 \\ 0 & 0 & a_1 & 1-3\varepsilon_1^{-1}a_1-\xi \end{pmatrix}$$

where a_i is the propensity for transfer from a chromophore in the ith shell to another, to which it is chemically bonded, in the $(i-1)^{\text{th}}$ shell (or to the core, if $i = 1$); ε_i is the ratio of efficiencies for inward and outward energy transfer between the same pair of chromophores (the latter usually expressible through eq. [27] as a simple function of the chromophore lineshapes and spectroscopic gradients). Lastly, ξ signifies losses associated with emission or irreversible energy utilization at the core. One advantage of the above representation is that it obviates any assumption of symmetry that chemical connectivity would suggest; this is a facet of particular relevance when issues of folding are to be entertained.

Fig. 8. Fifth-generation polyphenylether dendrimer, centred on a lanthanide ion such as Er^{3+} or Tb^{3+}. The threefold branching is formally described by a vertex degree $r = 3$. Such planar depictions misrepresent the three-dimensional folding that increasingly takes place with successive generations.

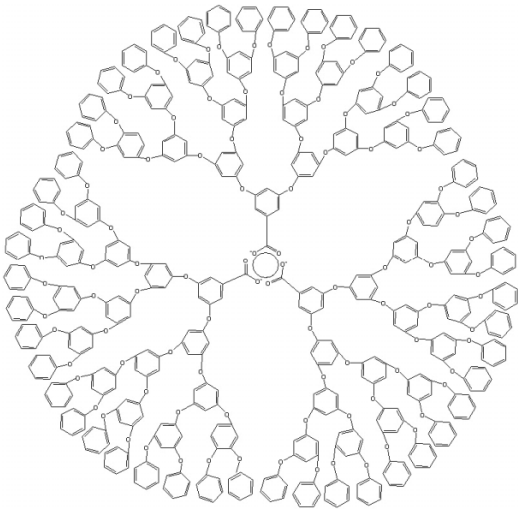

Results based on this model have already indicated a promising potential for representing the time-dependent energy flow towards the core, as indicated in Fig. 9*a*, lending a new capacity to interpret experimentally determined kinetic data in terms of physically meaningful quantities with a clear molecular interpretation. The significance of inter-shell directional transfer efficiency is readily exhibited by results such as that shown in Fig. 9*b*, where the increasingly strong dependence with successive generations of dendrimer growth are dramatically illustrated. In the more extensive results reported elsewhere (103), the effects of spectroscopic gradient and Stokes shift are also detailed.

In other recent developments of the theory based on molecular QED (104, 105), attention has become focused on optically "nonlinear" mechanisms for RET in dendrimers. Such mechanisms naturally fall into two classes: those in which two-photon absorption by individual donors is followed by a direct transfer of their acquired energy to an acceptor, and other processes wherein the excitation of two electronically distinct but neighbouring donor groups is followed by a collective migration of their energy to a suitable acceptor. These two types of transfer process are subject to markedly different forms of dependence on energy level structures, laser coherence factors, chromophore selection rules and architecture, possibilities for the formation of delocalized excitons, spectral overlap features, and the overall distribution of donors and acceptors. With such an array of measures to choose between, experimental differentiation of the mechanisms should prove relatively straightforward, and the first experimental results are awaited with keen interest.

5. Optical control of resonance energy transfer

A. Laser-assisted resonance energy transfer

The pace of development in nanofabrication techniques has promoted an increasing interest in the specific effects of

Fig. 9. (*a*) Extent of core excitation in a single-generation dendrimer of vertex degree ρ = 3, plotted as a function of time, for different values of the parameters *a*, ξ, and ε. (*b*) Core excited-state population (scaled by the number of chromophores) in dendrimers of vertex degree = 3, as a function of the inter-shell transfer efficiency, for third-, fourth- and fifth-generation dendrimers. Adapted from (103).

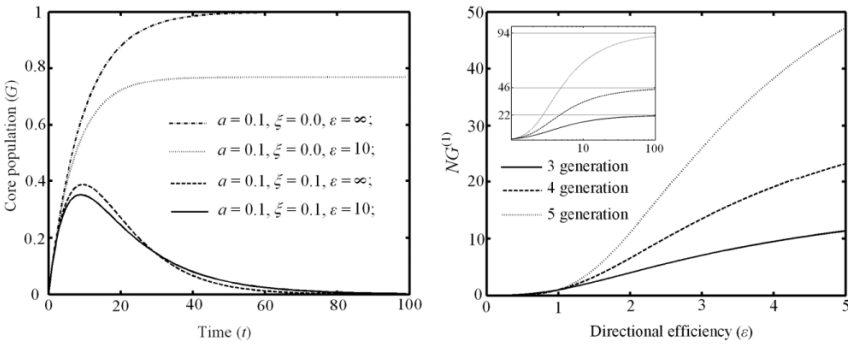

donor and acceptor placement in nanoscale geometries and periodic structures. However, the possibility of influencing the operation of RET by an optical field only recently began to receive notice. Specifically, attention has become focused on possible means to enhance energy transfer, or even switch it on and off, through the controlled input of an off-resonant, auxiliary beam of laser radiation, as schematically illustrated in Fig. 10. The first work in this area considered amplification effects that might be induced by such an auxiliary beam in systems where energy transfer will occur spontaneously (following initial excitation of the donors). It was shown that, at the levels of intensity currently available from mode-locked solid-state lasers, significant enhancements of the transfer rate could be expected (106). The discovery led to a coining of the term "LARET" to denote laser-assisted RET.

The quantum electrodynamical mechanism for LARET involves fourth-order time-dependent perturbation theory. Each interaction is linear in the electric field operator, see eq. [15], and thus entails the absorption or emission of a photon. Specifically, in addition to the two virtual photon events (creation and annihilation) of normal RET, this process involves the absorption and the stimulated re-emission of a photon from the throughput, off-resonant, laser light; each of these real photon events may also occur at either the donor or the acceptor. In general, all four of the resulting possible combinations contribute to the overall quantum amplitude; moreover, each has 24 different time-orderings associated with it. State-sequence representations (107, 108), such as the one illustrated in Fig. 11 (compare Fig. 4), represent a tractable basis for QED calculations that lead to the following eq. for the transfer probability at time *t*

$$[29]\qquad P(t) = \frac{\rho_f}{32\hbar c^2 \pi \varepsilon_0^4 R^6} \left| e_i \alpha_{lk}^{A}(-k')(\delta_{jk} - 3\hat{R}_j\hat{R}_k)\,\alpha_{lk}^{B}(k')\bar{e}_l + \bar{e}_i \alpha_{ij}^{A}(k')(\delta_{jk} - 3\hat{R}_j\hat{R}_k)\,\alpha_{lk}^{B}(-k')e_l \right|^2 \int_0^t I^2(t)\,\mathrm{d}t$$

Here, the α tensors are generalized polarizabilities (61) and $I(t)$ signifies the time-dependent pulses of irradiance delivered by the off-resonant beam; notice the recurrence of the characteristic short-range R^{-6} dependence on distance. Model calculations based on eq. [29] suggest that prominent departures from the normal kinetic behaviour of RET can be expected, as indicated in Fig. 12.

Fig. 10. General schematic of laser-assisted or optically controlled resonance energy transfer.

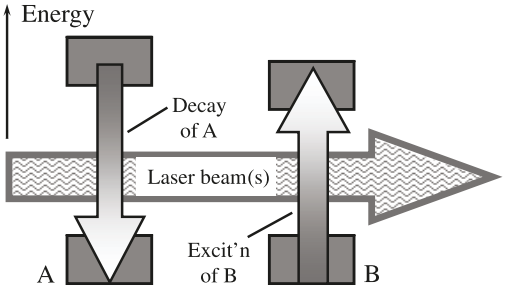

Fig. 11. One of four state-sequence diagrams for LARET. There are 24 pathways from the initial state on the left (excited *A*, ground state *B*) to the final state on the right left (ground state *A*, excited *B*), each progressing through three virtual intermediate states. In each case, ω denotes the off-resonant throughput radiation; in intermediate state boxes where the symbol is absent, a photon has been absorbed, while two ω symbols signify that stimulated emission has added an additional photon into the throughput. As with RET, ϕ denotes a virtual photon.

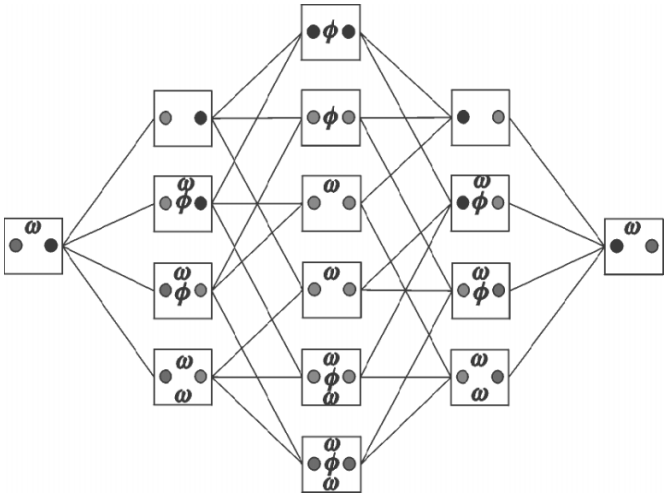

B. Optical switching in array devices

Recently, further interest has focused on structures that can be tailored to exploit the laser-assisted phenomenon. Specifically, consideration has been turned to systems in

Fig. 12. Profiles illustrating the effects of LARET on the kinetics of fluorescence, (*a*) from a donor and (*b*) acceptor, produced by introducing a square pulse of off-resonance laser radiation (dashed line) 100 ps after the initial donor excitation. The solid line shows the LARET behaviour, departing from the usual RET trace shown by the dotted segment. The pulse duration is 100 ps, and its intensity is 5×10^{12} W cm^{-2}. Adapted from (106).

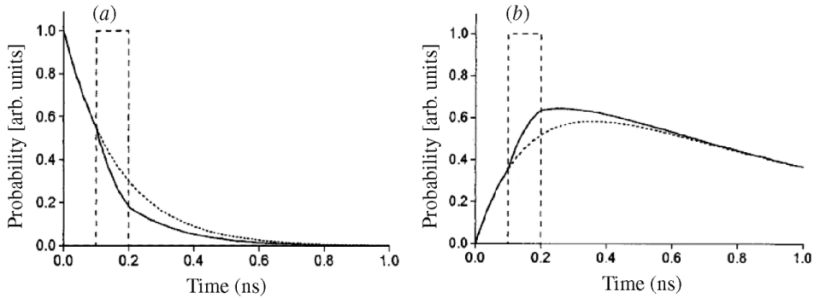

which each donor–acceptor pair has optical properties that satisfy the spectral overlap condition, but for which RET is designedly precluded by a customized geometric configuration (109). For example, as was observed in Section 3C, both short- and long-range RET is forbidden when the donor and acceptor undergo electric dipole transitions whose transition moments are perpendicular both to each other and also to the donor–acceptor displacement vector. For any such donor–acceptor pair, the LARET mechanism offers a means by which the throughput of non-resonant laser pulses can facilitate energy transfer when it would otherwise be rigorously forbidden. This optical switching of energy transfer, which has acquired the acronym OCRET (optically controlled resonance energy transfer), thus achieves the functionality of an optical transistor, with the electronic excitation representing a signal whose throughput is switched on by one or two auxiliary beams (110, 111).

The laser systems most capable of delivering the necessary levels of irradiance prove to be precisely those that will also offer directly controllable, ultrafast speeds of switching. Auspicious results have been obtained from detailed calculations on a prototype implementation of OCRET in planar nano-arrays (Fig. 13); results are illustrated by 3D plots in Fig. 14.

Fig. 13. Array implementation of OCRET: (*a*) overhead view of closely separated layers; the upper is a square-planar array of uniformly oriented donors, and the lower is a similarly constructed and registered array of acceptors. Black arrows represent donor transition dipoles in the upper layer, and grey arrows represent acceptor transition dipoles in the lower array; open arrows show an excited donor and its corresponding ground-state acceptor; (*b*) artist's impression of the view between the layers; the separation is exaggerated for clarity; (*c*) inter-layer depiction of the transition-moment orientations.

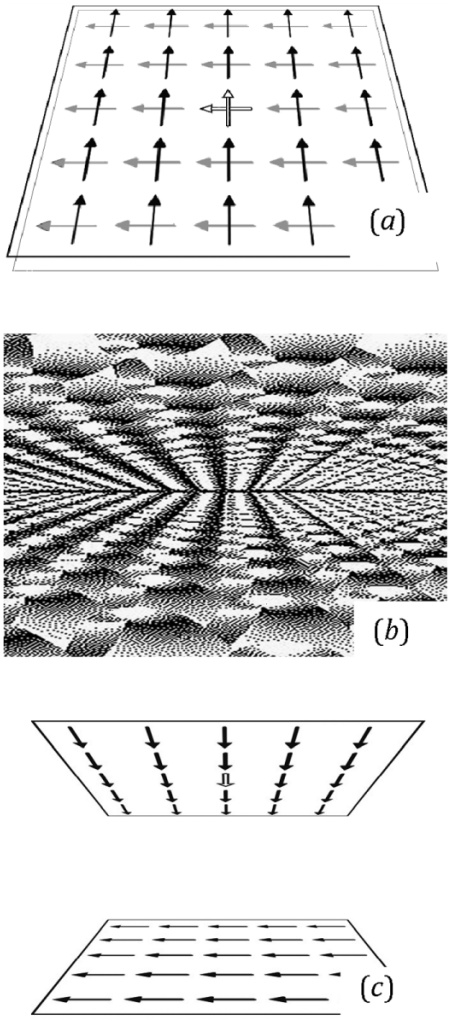

C. Implementation issues and applications

Results such as those shown in Fig. 14 encourage a view that the OCRET mechanism affords a realistic basis for a configuration of optical switches with parallel processing capability, operating without significant cross-talk. To address possible applications, a detailed analysis (112) has recently focused on the critical issue of transfer fidelity, defined as the efficiency of direct energy relocation, from an excited donor to its designated partner in the acceptor array, compared to the summed efficiencies for transfer to any other molecules within either array. The square-planar configuration proves to afford a significantly higher level of transfer fidelity than other likely contenders. It has also emerged that for optimal exploitation of the transition selection rules, the donor and acceptor molecules should belong to one of two common symmetry point groups, D_2 and C_{2v}. For such systems, through judicious choice of the relative values of the array spacing and lattice constant and the laser intensity, cross-talk can be driven down to arbitrarily low levels.

Generally, it may prove expedient to construct the donor and acceptor arrays as film layers, separated by a suitably

Fig. 14. Contour graphs depicting on a logarithmic scale the probability of energy transfer to the array of acceptors in the absence (left) and presence (right) of laser light. Efficiency of energy transfer is represented by the vertical scale, and dots indicate the locations of each acceptor.

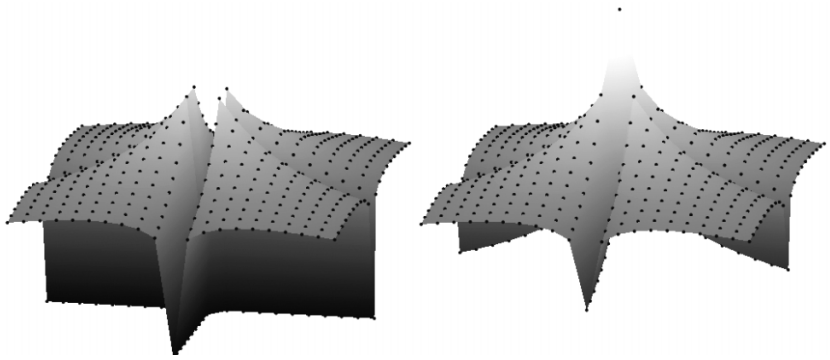

transparent ultra-thin spacer material. Organic dyes represent an extensive range of possibilities for the donor and acceptor species; the use of quantum dots is also conceivable, though their relative isotropy could make it difficult to preclude conventional RET unless spin-imprinted excitation and excitation transfer were to be engaged (113, 114). Two techniques that could offer promise for the deposition and tailoring of the molecular components in each active layer are dip-pen nanolithography and thermochemical nanolithography, in each of which the potential to order and chemically modify molecular units is now established (115–118).

The achievement of RET-based optical switching in an extensive parallel-processing unit introduces a number of potential applications beyond simple switching. The array results signify that, for example, pixel-based images, written by donor excitation, could be transferred with high fidelity to the acceptor film. In the realm of optical communications, possibilities might be built on the obvious capacity of such a system to act as an ultrafast information buffer; the high level of interest in such devices has already prompted others to explore "slow-light" methods, where a host of more problematic limitations apply (119, 120). In the longer term, OCRET may prove a significant channel of progress towards reliable systems for use in optical computing and communications routing.

6. Conclusion

Resonance energy transfer is a fundamental mechanism widely operative in complex multi-component systems. In this review, it has been shown how an increasingly diverse range of applications and devices can exploit features of the process, such as its dependence on the degree of spectral overlap between donor and acceptors, the sharp distance dependence, and transfer selectivity determined by the orientation of transition moments. Attention has been drawn to a number of novel schemes for the control and application of energy transfer, offering particularly bright new prospects for energy-harvesting and all-optical switching.

Acknowledgements

It is a pleasure to acknowledge the involvement of past and present members of my group in the unified theory developments at the University of East Anglia, and I gladly acknowledge their contributions. In particular, I must thank Philip Allcock, David Bradshaw, Richard Crisp, Gareth Daniels, Luciana Dávila Romero, Robert Jenkins, Gediminas Juzeliūnas, Justo Rodríguez, and Brad Sherborne. I gratefully acknowledge funding from the Engineering and Physical Sciences Research Council, the Leverhulme Trust, and the Royal Society.

References

1. V.M. Agranovich and M.D. Galanin. Electronic excitation energy transfer in condensed matter. Elsevier/North-Holland. Amsterdam, The Netherlands. 1982.
2. B.W. van der Meer, J. Coker, III, and S.-Y.S. Chen. Resonance energy transfer: theory and data. VCH. New York, NY, USA. 1982.
3. D.L. Andrews and A.A. Demidov (*Editor*s). Resonance energy transfer. Wiley. New York, NY, USA. 1999.
4. K. Sienicki. J. Chem. Phys. **94**, 617 (1991).
5. M.N. Berberan-Santos, J. Pouget, B. Valeur, J. Canceill, L. Jullien, and J.-M. Lehn. J. Phys. Chem. **97**, 11376 (1993).
6. M.R. Shortreed, S.F. Swallen, Z.-Y. Shi, W. Tan, Z. Xu, C. Devadoss, J.S. Moore, and R. Kopelman. J. Phys. Chem. B, **101**, 6318 (1997).
7. D.L. Andrews and R.G. Crisp. J. Fluorescence **16**, 191 (2006).
8. H. van Amerongen, L. Valkunas, and R. van Grondelle. Photosynthetic excitons. World Scientific. Singapore. 2000.
9. D.M. Guldi. Chem. Soc. Rev. **31**, 22 (2002).
10. M. Halim, J.N.G. Pillow, I.D.W. Samuel, and P.L. Burn. Synth. Metals, **102**, 922–923 (1999).
11. A.W. Freeman, S.C. Koene, P.L. Malenfant, M.E. Thompson, and J.M.J. Fréchet. J. Am. Chem. Soc. **122**, 12385 (2000).
12. T.D. Anthopoulos, J.P.J. Markham, E.B. Namdas, J.R. Lawrence, I.D.W. Samuel, S.-C. Lo, and P.L. Burn. Org. Electronics **4**, 71 (2003).
13. P. Furuta, J. Brooks, M.E. Thompson, and J.M.J. Fréchet. J. Am. Chem. Soc. **125**, 13165 (2003).
14. P.L. Burn, S.-C. Lo, and I.D.W. Samuel. Adv. Mater. **19**, 1675 (2007).
15. T. Miyakawa and D.L. Dexter. Phys. Rev. B, **1**, 70 (1970).
16. F. Auzel. J. Lumin. **45**, 341 (1990).
17. M. Chua and P.A. Tanner. J. Lumin. **66–7**, 203 (1995).
18. D.L. Andrews. J. Raman Spectrosc. **31**, 791 (2000).
19. D.L. Andrews and R.D. Jenkins. J. Chem. Phys. **114**, 1089 (2001).

20. B.W. Lovett, J.H. Reina, A. Nazir, B. Kothari, and G.A. Briggs. Phys. Lett. A, **315**, 136 (2003).
21. A.O. Govorov. Phys. Rev. B, **68**, 075315 (2003).
22. S. Sangu, K. Kobayashi, A. Shojiguchi, and M. Ohtsu. Phys. Rev. B, **69**, 115334 (2004).
23. P.R. Selvin. Nature Struct. Biol. **7**, 730 (2000).
24. S. Hohng, C. Joo, and T. Ha. Biophys. J. **87**, 1328 (2004).
25. S. Rüttinger, R. Macdonald, B. Krämer, F. Koberling, M. Roos, and E. Hildt. Biomedical Optics, **11**, 024012 (2006).
26. S.V. Koushik, H, Chen, C. Thaler, H.L. Puhl, III, and S.S. Vogel. Biophys. J. **91**, L99 (2006).
27. G. Boas. Biophotonics Int. **14** (2) 30 (2007).
28. J. Zhang and M.D. Allen. Mol. Biosystems, **3**, 759 (2007).
29. E.A. Jares-Erijman and T.M. Jovin. Nature Biotechnol. **21**, 1387 (2003).
30. M. Elangovan, H. Wallrabe, Y. Chen, R.N. Day, M. Barroso, and A. Periasamy. Methods, **29**, 58 (2003).
31. S.K. Sekatskii. Phil. Trans. R. Soc. A – Math. Phys. Eng. Sci. **362**, 901 (2004).
32. J.P.S. Farinha and J.M.G. Martinho. Springer Ser. Fluoresc. **4**, 215 (2008).
33. V. Bagalkot, L. Zhang, E. Levy-Nissenbaum, S. Jon, P.W. Kantoff, R. Langer, and O.C. Farokhzad. Nano Lett. **7**, 3065 (2007).
34. I.L. Medintz, A.R. Clapp, H. Mattoussi, E.R. Goldman, B. Fisher, and J.M. Mauro. Nature Materials, **2**, 575 (2003).
35. H. Zhang and D.M. Rudkevich. Chem. Commun. 1238 (2007).
36. X. Fan, A. Majumder, S.S. Reagin, and E.L. Porter. J. Biomed. Opt. **12,** 03407 (2007).
37. T. Förster. Annalen. Phys. **2**, 55 (1948).
38. S.A. Latt, H.T. Cheung, and E.R. Blout. J. Am. Chem. Soc. **87**, 995 (1965).
39. D.L. Andrews and J. Rodríguez. J. Chem. Phys. **127**, 084509 (2007).
40. A.A. Demidov and D. L. Andrews. *In* Encyclopedia of chemical physics and physical chemistry. Vol. 3. J. H. Moore and N. D. Spencer (*Editor*s). Institute of Physics. Bristol. 2001. pp. 2701–2715.
41. C. Galli, K. Wynne, S.M. Lecours, M.J. Therien, and R.M. Hochstrasser. Chem. Phys. Lett. **206**, 493 (1993).
42. B.W. van der Meer. *In* Resonance energy transfer. D.L. Andrews and A.A. Demidov (*Editors*). Wiley. New York, NY, USA. 1999. pp. 151–172.
43. C.G. dos Remedios and P.D.J Moens. J. Struct. Biol. **115**, 175 (1995).
44. G. Ramanoudjame, M. Du, K.A. Mankiewicz, and V. Jayaraman. Proc. Natl. Acad. Sci. USA. **103**, 10473 (2006).
45. X. You, A.W. Nguyen, A. Jabaiah, M.A. Sheff, K.S. Thorn, and P.S. Daugherty. Proc. Natl. Acad. Sci. USA. **103**, 18458 (2006).
46. P.R. Selvin. Annu. Rev. Biophys. Biomol. Struc. **31**, 275 (2002).
47. B. Schuler. Chem. Phys. Chem. **6**, 1206 (2005).
48. F. Tanaka. J. Chem. Phys. **109**, 1084 (1988).
49. Z.G. Yu. J. Chem. Phys. **127**, 221101 (2007).
50. M. Isaksson, N. Norlin, P.-O. Westlund, and L.B.-Å. Johansson. Phys. Chem. Chem. Phys. **9**, 1941 (2007).
51. J.R. Lakowicz. Principles of fluorescence spectroscopy. 2nd ed. Kluwer Academic. New York, NY, USA. 1999. Chap. 10.
52. B. Valeur. Molecular fluorescence. Principles and aapplications. Chapter 9. Wiley-VCH. Weinheim, Germany. 2002.
53. D.L. Dexter. J. Chem. Phys. **21**, 836 (1953).
54. G.D. Scholes and K.P. Ghiggino. J. Phys. Chem. **98**, 4580 (1994).
55. E.K.L. Yeow and K.P. Ghiggino. J. Phys. Chem. A, **104**, 5825 (2000).
56. D.L. Andrews and T. Thirunamachandran. J. Chem. Phys. **67**, 5026 (1977).
57. W.L. Levshin. Z. Angew. Phys. **32**, 307 (1925).
58. F. Perrin. Ann. de Phys. **12**, 169 (1929).
59. G.D. Scholes and D.L. Andrews. J. Chem. Phys. **107**, 5374 (1997).
60. A. Salam. J. Chem. Phys. **122**, 044112 (2005).
61. D.P. Craig and T. Thirunamachandran. Molecular quantum electrodynamics. Dover. New York, NY, USA. 1998.
62. R.G. Woolley. Int. J. Quantum Chem. **74**, 531 (1999).
63. P.W. Milonni. The quantum vacuum. Academic Press. Boston, MA. 1994.
64. R.G. Woolley. Proc. R. Soc. London, Ser A, **456**, 1803 (2000).
65. J.S. Avery. Proc. Phys. Soc. **88**, 1 (1966).
66. L. Gomberoff and E.A. Power. Proc. Phys. Soc. **88**, 281 (1966).
67. D.L. Andrews. Chem. Phys. **135**, 195 (1989).
68. G.J. Daniels, R.D. Jenkins, D.S. Bradshaw, and D.L. Andrews. J. Chem. Phys. **119**, 2264 (2003).
69. D.L. Andrews and B.S. Sherborne. J. Chem. Phys. **86**, 4011 (1987).
70. G. Juzelinas and D.L. Andrews. Adv. Chem. Phys. **112**, 357 (2000).
71. L. Novotny and B. Hecht. Principles of nano-optics. University Press, Cambridge, UK. 2006. pp. 285–293.
72. R.D. Jenkins, G.J. Daniels and D.L. Andrews. J. Chem. Phys. **120**, 11442 (2004).
73. M.N. Berberan-Santos, E.J.N. Pereira and J.M.G. Martinho. J. Chem. Phys. **107**, 10480 (1997).
74. D. L. Andrews and G. Juzeliūnas. J. Chem. Phys. **95**, 5513 (1991).
75. G.D. Scholes, C. Curutchet, B. Mennucci, R. Cammi, and J. Tomasi. J. Phys. Chem. B, **111**, 6978 (2007).
76. C. Curutchet, G.D. Scholes, B. Mennucci, and R. Cammi. J. Phys. Chem. B, **111**, 13253 (2007).
77. G. Juzeliūnas and D.L. Andrews. Phys Rev. B, **49**, 8751 (1994).
78. D.L. Andrews and G. Juzelinas. J. Chem. Phys. **96**, 6606 (1992).
79. C. Devadoss, P. Bharathi, and J.S. Moore. J. Am. Chem. Soc. **118**, 9635 (1996).
80. X. Hu and K. Schulten. Phys. Today, **50** (8) 28 (1997).
81. R. van Grondelle and V. Novoderezhkin. Biochem. **40**, 15057 (2001).
82. T. Renger, V. May, and O. Kühn. Phys. Rep. **343**, 138 (2001).
83. R.J. Cogdell, A. Gall, and J. Kohler. Quart. Rev. Biophys. **39**, 227 (2006).
84. T. Brixner, J. Stenger, H.M. Vaswani, M. Cho, R.E. Blankenship, and G.R. Fleming. Nature (London, UK), **434**, 625 (2005).
85. G.S. Engel, T.R. Calhoun, E.L. Read, T.-K. Ahn, T. Mancal, Y.-C. Cheng, R.E. Blankenship, and G.R. Fleming. Nature (London, UK), **446**, 782 (2007).
86. P. Ball. Nanotechnol. **13**, R15 (2002).
87. D.L. Andrews. *In* Introduction to complex mediums for optics and electromagnetics. W.S. Weiglhofer and A. Lakhtakia (*Editors*). SPIE. Bellingham, WA, USA. 2003. pp 141–163.
88. D.L. Andrews (*Editor*). Energy harvesting materials. World Scientific. Singapore. 2005.
89. A. Bar-Haim, J. Klafter, and R. Kopelmann. J. Am. Chem. Soc. **119**, 6197 (1997).
90. A. Archut and F. Vögtle. Chem. Soc. Rev. **27**, 233 (1998).

91. A. Adronov and J. M. J. Fréchet. Chem. Commun. 1701 (2000).
92. A. Nantalaksakul, D.R. Reddy, C.J. Bardeen, and S. Thayumanavan. Photosynth. Res. **87**, 133 (2006).
93. C. Devadoss, P. Bharathi, and J.S. Moore. J. Am. Chem. Soc. **118**, 9635 (1996).
94. S.F. Swallen, Z.-Y. Shi, W. Tan, Z. Xu, J.S. Moore, and R. Kopelman. J. Lumin. **76–7**, 193 (1998).
95. P.G. van Patten, A.P. Shreve, J.S. Lindsey, and R.J. Donohoe. J. Phys. Chem. B, **102**, 4209 (1998).
96. M. Nakano, M. Takahata, H. Fujita, S. Kiribayashi, and K. Yamaguchi. Chem. Phys. Lett. **323**, 249 (2000).
97. J.L. Bentz and J.J. Kozak. J. Lumin. **121**, 62 (2006).
98. A. Blumen, A. Volta, A. Jurjiu, and Th. Koslowski. Physica A, **356**, 12 (2005).
99. S.M. Vlaming, D.J. Heijs, and J. Knoester. J. Lumin. **111**, 349 (2005).
100. D. Rana and G. Gangopadhyay. J. Chem. Phys. **11**8 434 (2003).
101. D.L. Andrews and S. Li. *In* Nanomodeling II. A. Lakhtakia and S.A. Maksimenko (*Editors*). Proc. SPIE **6328**, 63280V (2006).
102. D.L. Andrews and S. Li. Chem. Phys. Lett. **433**, 239 (2006).
103. D.L. Andrews, S. Li, J. Rodríguez, and J. Slota. J. Chem. Phys. **127**, 134902 (2007).
104. D.L. Andrews and D.S. Bradshaw. J. Chem. Phys. **121**, 2445 (2004).
105. D.L. Bradshaw and D.L. Andrews. Chem. Phys. Lett. **430**, 191 (2006).
106. P. Allcock, R.D. Jenkins, and D.L. Andrews. Phys. Rev. A, **61**, 023812 (2000).
107. R.D. Jenkins, D.L. Andrews, and L.C. Dávila Romero. J. Phys. B: Atom. Molec. Opt. Phys. **35**, 445 (2002).
108. B.W. Alligood and A. Salam. Mol. Phys. **105**, 395 (2007).
109. D.L. Andrews and R.G. Crisp. J. Opt. A: Pure Appl. Opt. **8**, S106 (2006).
110. D.L. Andrews, R.G. Crisp, and S. Li. J. Chem. Phys. **127**, 174702 (2007).
111. D.L. Andrews. Phys. Rev. Lett. **99**, 023601 (2007).
112. D.S. Bradshaw and D.L. Andrews. J. Chem. Phys. **128**, 144506 (2008).
113. B.W. Lovett, J.H. Reina, A. Nazir, and G.A.D. Briggs. Phys. Rev. B, **68**, 205319 (2003).
114. G.D. Scholes and D.L. Andrews. Phys. Rev. B, **72**, 125331 (2005).
115. R.D. Piner, J. Zhu, F. Xu, S.H. Hong, and C.A. Mirkin. Science (Washington, DC), **283**, 661 (1999).
116. C.A. Mirkin, S.H. Hong, and L. Demers. Chem. Phys. Chem. **2**, 37 (2001).
117. N.P. Reynolds, S. Janusz, M. Escalante-Marun, J. Timney, R.E. Ducker, J.D. Olsen, C. Otto, V. Subramaniam, G.J. Leggett, and C.N. Hunter. J. Am. Chem. Soc. **129**, 14625 (2007).
118. R. Szoszkiewicz, T. Okada, S.C. Jones, T.D. Li, W.P. King, S.R. Marder and E. Riedo. Nano Lett. **7**, 1064 (2007).
119. R.W. Boyd and P. Narum. J. Mod. Opt. **54**, 2403 (2007).
120. K.L. Tsakmakidis, A.D. Boardman, and O. Hess. Nature (London, UK), **450**, 397 (2007).